Available online at www.sciencedirect.com

SciVerse ScienceDirect

Ceramics International 39 (2013) 1307–1313

CERAMICS INTERNATIONAL

www.elsevier.com/locate/ceramint

Yb^{3+} doped Lu_2O_3 transparent ceramics by spark plasma sintering

Mythili Prakasam[a,*], Oudamsack Viraphong[a], Dominique Michau[a], Philippe Veber[a], Matias Velázquez[a], Kiyoshi Shimamura[b], Alain Largeteau[a]

[a]*Institut de Chimie de la Matière Condensée de Bordeaux-CNRS, Bordeaux 33608, France*
[b]*National Institute for Materials Science (NIMS), Tsukuba 305-0044, Japan*

Received 25 April 2012; received in revised form 13 July 2012; accepted 18 July 2012
Available online 25 July 2012

Abstract

Transparent ceramics of 10% Yb doped Lu_2O_3 was fabricated by spark plasma sintering. The operating vital parameters in yielding transparency and mutual effects of sintering, pressure, dwell time, heating rate and annealing temperature on microstructure have been investigated. Fully compacted specimens were obtained at 1250 °C and the average grain size increased from few nm up to 5 μm until 1700 °C, above which abnormal grain growth was witnessed. The post-annealing of sintered ceramics at 1200 °C removes discoloration and improves transparency. The ceramics prepared at 1700 °C with dwell time of 5 min and heating rate at 50 °C/min shows the maximum transmittance with a thickness of 2 mm of 55% at a wavelength of 2 μm.

Keywords: A. Grain growth; A. Sintering; B. Grain size; B. Grain boundaries

1. Introduction

Lu_2O_3 is a sesquioxide with cubic crystal structure which has applications in scintillation detectors and laser gain media. Invention of solid state lasers led to tremendous efforts to obtain high quality laser gain materials, in particular through single crystals. In the last decade, transparent ceramics processed with nanosized ceramic powders and advanced densification technology provides an alternative approach to overcome the disadvantages/limits of conventional single-crystal growth methods. It would be much easier to elaborate polycrystalline ceramics with a full densification state and a homogeneous chemical composition under sintering temperature much lower than its melting point with relatively low cost and size flexibility. Amongst the existing sintering techniques spark plasma sintering (SPS) is preferred for its simplicity in usage and rapid sintering. The control of defects is achieved by optimizing the sintering parameters and the quality of starting powder. Recently, an impressive 140 W power scaling was achieved in a single passively mode locked thin disk laser cavity with diode pumping at 976 nm with $Yb:Lu_2O_3$ single crystals grown by the heat exchanger method, outperforming the well known Yb:YAG crystal performances under this excitation scheme [1]. So, currently, $Lu_2O_3:Yb^{3+}$ crystals exhibit a potential to replace Yb^{3+}:YAG for 976 nm diode pumped high-power laser applications especially because of their excellent thermal conductivity when doped optimally with Yb^{3+} ions [2–5]. In addition, in rare-earth sesquioxide single crystals, Yb^{3+} ions have an emission band which is twice broader than that of Yb:YAG crystals, making them potentially interesting as gain media for ultrafast laser systems [15].

In order to get sufficient absorption of the pump radiation in the thin crystal plates (on the order of 200 μm), moderately high Yb concentrations are necessary, and an optimum level of doping must be found between self-quenching and self-trapping mechanisms to maintain the emission lifetime of Yb^{3+} ions at its highest level. It was recently demonstrated by Sanghera et al. [6], that laser

*Corresponding author. Tel.: +33 540008951; fax: +33 540002761.
E-mail addresses: prakasam@icmcb-bordeaux.cnrs.fr, mythili.prakasam@gmail.com (M. Prakasam).

0272-8842/$ - see front matter © 2012 Elsevier Ltd and Techna Group S.r.l. All rights reserved.
http://dx.doi.org/10.1016/j.ceramint.2012.07.065

oscillation can be obtained at 1081 nm using a 10% Yb^{3+}-doped Lu_2O_3 ceramic made by hot pressing. Further output power of 2.5 W was obtained with an optical-to-optical efficiency of ~10% representing the highest output power achieved and the highest concentration of Yb^{3+} used thus far in an Yb^{3+}-doped Lu_2O_3 ceramic. Although these laser performances remain very modest in comparison with the average power and highest laser slope achieved in single crystals by Petermann and Baer [1,7], as well as with the CW laser output of 72 W at 1.064 μm obtained with YAG ceramic rod [29], we chose 10% Yb doped Lu_2O_3 in order to compare the benefits of recently published work by Sanghera et al. [6] by the hot pressing method with SPS.

Various approaches have been tried by researchers, such as sol–gel, chemical wet process and co-precipitation to produce different ceramic oxide powder [8–10]. In the present work, due to the commercial non-availability of Yb^{3+} doped Lu_2O_3 powder; co-precipitation was preferred to produce the nanosized powders.

In the recent years, spark plasma sintering (SPS) has been widely opted for fabricating opto-ceramics and piezo-ceramics instead of conventionally used hot-isostatic pressing (HIP) or vacuum sintering at high temperatures. SPS is mostly favored for compaction of ceramics and metals to a dense body in a short time, usually within a few minutes [11]. Recently, highly transparent ceramics with controlled microstructures have been prepared by a two-step pressure profile, i.e., a low pre-loading pressure at low temperatures and a high pressure at high temperatures [12]. The heating rate is another important sintering parameter for densification in the second and third stages. Although a fast heating rate >30 °C/min is widely used in SPS, a low heating rate was applied to fabricate highly transparent Al_2O_3 [13] and $MgAl_2O_4$ [14]. The SPS yielded polycrystalline oxides generally fails to yield transmittance expected by theoretical inline transmittance, especially in the ultraviolet and low visible wavelengths. This optical behavior may be principally due to the presence of pores that are often observed at the grain junctions of the ceramics subjected to SPS but also due to the reduction conditions arising from the presence of graphite at high temperature in vacuum. The combination of the two-step profile and low heating rate can be more advantageous to obtain fine microstructure bodies with improved transparencies. Our research team recently reported the possibility of growing Yb^{3+}-doped Y_2O_3 and Lu_2O_3 single crystals by a flux method in air and at half of their melting temperature, hence stabilizing directly the Yb^{3+} oxidation state and preventing the formation of Yb^{3+} pairs, likely to reduce the quantum yield by cooperative luminescence, even at the optimum concentration required for high-power laser application [15]. Although the flux method has been turned into an industrial process by several companies around the world, the minimum complexity in the processing and short time consumption of SPS techniques led us to probe it simultaneously on the YLO ceramics. In the present work, we study about the various parameters catered to yield good quality transparent ceramic of YLO, with short processing time.

2. Experimental procedure

2.1. Synthesis of YLO powder

10% Yb^{3+} doped Lu_2O_3 powder was synthesized by the co-precipitation method. Lu_2O_3 (99.99%), Yb_2O_3 (99.99%), Nitric acid (99.999%), Ammonium hydroxide (99.99%) and Acetone (AR grade) were procured from Alfa Aesar. Stoichiometric amounts of starting powders were mixed in hot diluted HNO_3 to obtain Lu and Yb precursor forming the nitrate precursor mixture, which was added to NH_4OH to form the precipitate at a pH value of 9. Then the precipitate was dried in an oven at 100 °C for 2 h, followed by grinding the precipitate and calcination at 600 °C in air for 12 h. The calcined powder was ball milled with ethanol for 48 h. The final product was analyzed with powder X-ray diffraction (XRD) to confirm the formation of YLO. The grain size was observed to be around 1 nm by Scanning Electron Microscopy (SEM).

2.2. Ceramic fabrication and characterization

For each experiment 2 g of synthesized powder was filled into a graphite die having an inner diameter of 8 mm. The graphite die was covered with a thermal insulator carbon fiber to avoid contamination from the graphite die to the starting powder. An optical pyrometer was used to measure the temperature of the graphite die surface. The graphite mould was placed in SPS operating chamber (DR. SINTER LAB spark plasma sintering system, Model SPS-511S/ SPS-515S) under vacuum of 10^{-3} Torr. The pulse sequence for the SPS applied voltage for all the samples was 12:2 (i.e. 12 ON/2 OFF). The shrinkage of the densifying powder was continuously monitored by the displacement of the punch rod. The temperature was first increased to 600 °C within 3 min and then increased to a range of temperatures from 1400 °C to 1800 °C with different heating rate (R_H) ranging from 5 °C/min to 200 °C/min and dwell time. Uniaxial pressures ranging from 40 MPa to 100 MPa were applied at room temperature (T_R) and sintering temperatures (T_S) and their significances have been analyzed. The cooling rate (R_C) and R_H were maintained equal in all the experiments. The higher value of R_H and higher value of R_C lead to opacity and cracking of the ceramics, respectively. The SPS ceramics obtained were black in color, due to the reducing nature of the experimental process and porosity. The thermal insulator layer on the ceramics was removed and the ceramic was annealed at 900 °C for 1 h in air to compensate the lost oxygen during the course of experiment. Then the ceramics were mirror polished on both sides using diamond slurry. The thickness of the ceramics

after polishing was approximately 3 mm. Powder X-ray diffraction (XRD) analyses were performed with a PANalytical X'pert MDP diffractometer with θ–θ Bragg Brentano configuration with a backscattering graphite monochromator for K_α Cu radiation working at 40 kV and 40 mA. The density was measured by the Archimedes method in distilled water. The microstructure was observed by a scanning electron microscope (Jeol 840 SEM). The optical transmittance spectrum was measured by using a double beam spectrophotometer (Varian Cary 5000) at a range of between 200 and 3000 nm.

3. Results and discussion

3.1. Powder X-ray diffraction and density measurements of YLO ceramics

Fig. 1 shows XRD patterns of the 10% Yb-doped Lu_2O_3 starting powder obtained after calcination for 12 h at 600 °C in air and YLO ceramics sintered at various temperatures and dwell time. The unit cell parameters of the cubic crystal structure of Lu_2O_3 and Yb_2O_3 are $a=10.390$ Å and 10.435 Å, respectively. In the present study, we obtained the unit cell parameter for YLO as $a=10.402$ Å, indicating a slight increase than the value of Lu_2O_3 cell parameter, due to the incorporation of the Yb in the crystal structure of Lu_2O_3. The obtained value is in agreement with that reported in literature [16]. We observed that in the whole temperature range (1400–1800 °C) of analyses chosen for investigation, no additional phases or decompositions have been observed. The density was measured by the Archimedes method in distilled water. The theoretical density was calculated to be 9.3827 g/cm^3. All the specimens had relative densities greater than 99.5%. With the increase in T_S and P_S, a gradual increase in the value of density was observed.

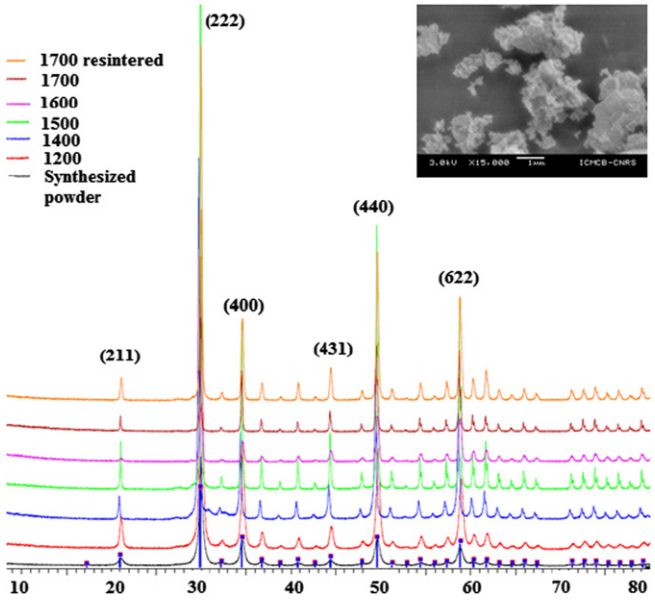

Fig. 1. Powder X-ray diffraction patterns of synthesized starting powder and various ceramics fabricated at different sintering temperatures. Inset shows grain size of the starting powder.

3.2. Optimizing the sintering parameters for fabrication of transparent YLO ceramics

3.2.1. Effect of applied pressure

Among the various vital parameters determining the transparency of ceramics, grain size, grain-boundary phase and pores play a pivotal role. Irrespective of the grain size, provided that the residual pores are free, higher transmittance of the ceramic has been obtained [17]. Fig. 2 shows the dependence of density on the sintering temperature. We observed that sintering curves of the YLO bodies are strongly dependent on the preload pressure (P_o) i.e., $t=0$. P_o influences initial packing density significantly resulting in increase of packing density manifold. There is a descending shift in the initial densification on ascending P_o. We observed the variation of the densification (1) by applying constant maximum pressure (P_S) in the entire process and (2) by applying P_S during the dwell time (t_s). Notable increase in densification was observed, when $P_o=P_S$. The increase in densification can be justified as follows: The applied pressure has a direct effect on particle rearrangement and agglomerations, paving way to an increase in compaction in the first sintering stage. High pressure also accelerates densification by plastic deformation leading to second sintering stage [18,19]. We observed that after the pressure was increased to 100 MPa, the relative density gradually reached above 95% with increasing t and T_S. Densification in the saturated densification might be mainly due to grain boundary diffusion associated with the grain growth.

3.2.2. Effect of sintering temperature

The complete densification of the ceramics not only relies on P_o or P_S, but on the grain growth as well, which in turn is dependent on T_S. In the YLO ceramics, we observed that the maximum densification was reached at 1250 °C, above this temperature, the densification remains stable. In general, when a complete dense body is held at

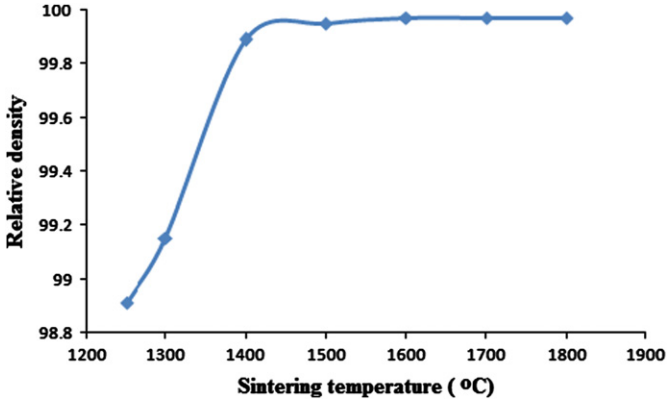

Fig. 2. Dependence of relative density on sintering temperature at $P_S=100$ MPa, $t_s=5$ min.

high temperature for long time, it usually results in the grain growth. In the present case, we have to tune down the average size of the grain approaching tens to hundreds of micrometers. Also large grained materials exhibit poor mechanical strength in comparison to the small grain sized materials. Though the report [18] has shown that laser oscillation was demonstrated in the relatively large grain size of ~50 μm, still large grained materials cannot render efficiency demanding high thermal shock resistance, such as high energy laser systems that can generate massive heat loads. Further to improve the first stage of sintering between grains, the nanosized grain is desired. Chen et al. [20,21] suggested two-stage sintering based on thermodynamical point of view. Accordingly, there is an active temperature range which enlivens grain boundary diffusion, but mildly slugging grain boundary migration hence leading to further densification without any significant grain growth. We implemented the following methodology $T_R \rightarrow T_S \rightarrow T_S + 100\ ^\circ C\ (t_s = 0) \rightarrow T_S$ to control the grain growth. The average grain sizes were differing over a range of 10 nm to 5 μm.

3.2.3. Effect of heating rate

We observed that the formation of pores and size distribution of the grain are strongly influenced by R_H. Even though when at higher $R_H > 50\ ^\circ C/min$, P_S effects on yielding higher densification at the end stage of sintering, pores were observed at the triple junctions of grain boundaries. The number of pores increased with $R_H > 50\ ^\circ C/min$. The average size of the grain increases rapidly with increasing R_H, leading to inhomogeneous grain size distribution inhibiting transparency of the ceramic. Large stress formed among the grains leads to inhomogeneous and large average grain size at higher R_H [22]. In YLO ceramics, we observed that the formation of pore and increase of grain size is predominant at $R_H > 50\ ^\circ C/$ min and as well as at $R_H < 50\ ^\circ C/min$, irrespective of t_s. The optimal R_H to yield transparent YLO ceramics was determined to be $R_H = 50\ ^\circ C/min$. There are similar reports [23–27] on Al_2O_3 ceramics prepared by SPS ascertaining a possibility of grain boundary diffusion and creep densification, yielding smaller grain growth at higher R_H than at lower R_H. Aforesaid is valid for YLO at $R_H > 50\ ^\circ C/$ min. Whereas in the regime, when $R_H < 50\ ^\circ C/min$ for YLO, the lower the R_H greater the larger grain growth, a similar trend has been reported [28] for Y_2O_3 ceramics prepared by SPS. We further observed that the crack is not observed in the sintered samples with $R_H = R_C$. In the case of lower R_H and higher R_C or vice versa, there is a crack on the surface of the sintered body.

3.2.4. Effect of post-annealing temperature

In general most of the SPS fabricated ceramics such as ZrO_2, Al_2O_3 and $MgAl_2O_4$ exhibit a grayish discoloration. The discoloration can be attributed to the defects, mainly oxygen vacancies formed [24] during SPS, due to the reduced atmosphere. The discoloration deepens at higher R_H, suggesting a higher defect concentration. A higher concentration of defects accelerates the grain growth during sintering [26]. In the present study, all the sintered YLO ceramics were annealed at 1200 °C for 12 h. During the annealing process, oxygen vacancies are compensated, resulting in its colorlessness and also enhancing its transparency, particularly in the visible range. When the annealing temperature is increased above 1200 °C, it leads to opacification of the ceramics due to the increase in porosity and abnormal grain growth.

3.2.5. Transparency of YLO ceramics

Fig. 3 shows the photographs of transparent YLO ceramics sintered at $P_S = 100$ MPa, $R_H = 50\ ^\circ C/min$, $T_S = 1700\ ^\circ C$ ($t_s = 5$ min) and 1400 °C ($t_s = 20$ min) with post annealing at 1200 °C for 12 h. The printed texts 30 mm below the ceramic wafers were readable, exhibiting high transparency. All the ceramics fabricated were slightly gray in color. The color gradually lightens with increase in temperature. The samples sintered at 1700 °C for 5 min exhibited comparatively higher transparency (Fig. 4) than that of the ceramics sintered at 1400 °C. The increasing transmission with sintering temperature may be attributed due to densification. Further even though the maximum compaction is achieved at 1400 °C, the feasibility of homogenous grain distribution occurs at increasing temperature. This could be another justification for the maximum transparency obtained at higher temperatures. Although the porosity measured by Archimedes principle indicates that it remains constant above 1250 °C, it is considered that additional densification continued to occur

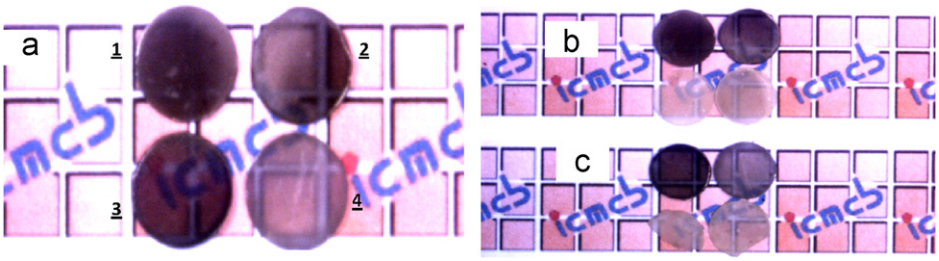

Fig. 3. 10% Yb_2O_3 doped Lu_2O_3 ceramics fabricated at (a) 1. $R_H = 10\ ^\circ C/min$, 1700 °C and $t_s = 20$ min and $P_S = 100$ MPa, 2. $R_H = 10\ ^\circ C/min$, 1700 °C and $t_s = 5$ min and $P_S = 100$ MPa, 3. $R_H = 50\ ^\circ C/min$, 1700 °C and $t_s = 20$ min and $P_S = 100$ MPa, and 4. $R_H = 50\ ^\circ C/min$, 1700 °C and $t_s = 5$ min and $P_S = 100$ MPa. (b and c) The corresponding samples compared with annealed samples at 1200 °C for 12 h for samples shown in (a).

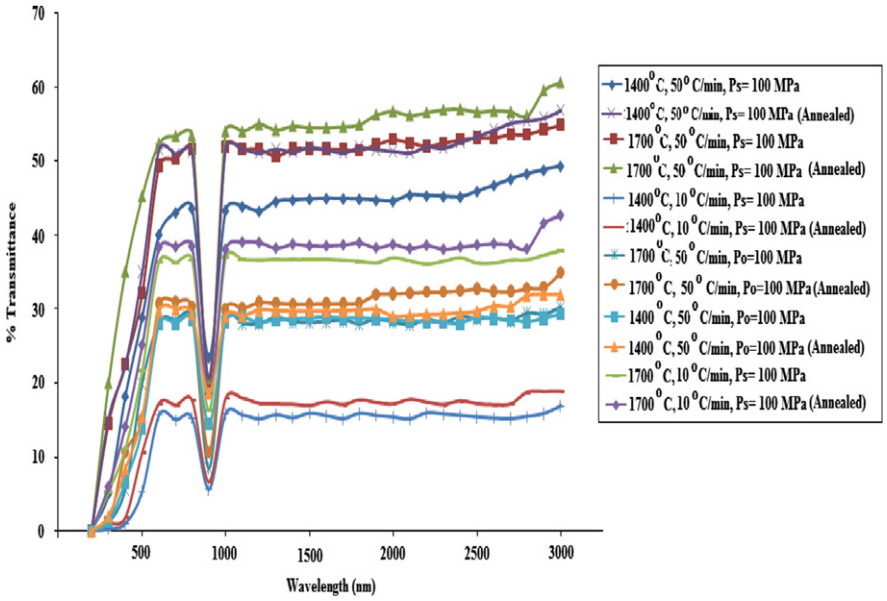

Fig. 4. Transmittance spectrum of 10% Yb doped Lu_2O_3 ceramics fabricated with various sintering parameters.

gradually at higher temperatures. With slight changes in density at higher temperatures leads to increased transmittance at higher temperatures, being insensitive to porosity. When $R_H > 50$ °C/min, the transmittance decreases rapidly in visible and infrared range irrespective of the P_o and P_S. At $R_H < 50$ °C/min < 10 °C/min, the transmittance increases gradually with $P_o = P_S$. However $R_H < 10$ °C/min leads to a sudden decline in transmittance, owing to the abnormal grain growth and residual porosity. The YLO ceramics fabricated at 1700 °C and 1400 °C had nearly 5–10% improvement in transmittance upon annealing at 1200 °C for 12 h. The discoloration disappears at annealing temperature of 1200 °C, compensating the oxygen vacancies, being the optimal temperature for post-annealing YLO ceramics.

The SEM micrographs in Fig. 5, show the dynamics of microstructure in YLO ceramics. We observed that the average grain size decreases with increasing P_S. HIP and vacuum sintering at high temperatures are touted to yield optically transparent ceramics in comparison to SPS, especially in the UV and lower visible wavelengths. But in the present investigation, we obtained nearly the same transmittance as that was reported for HIP yielded YLO ceramics, with add on benefits like comparatively lesser temperature and short processing time. In general, residual pores which are in the same size range as the incident wavelength act as an efficient scattering source at a corresponding wavelength. We have noted that the apparent porosity of YLO ceramics decreases with increasing temperatures and increasing holding time, while the applied pressure has little effect on the porosity because of the high hardness. There is a slight decline in porosity, when $R_H > 10$ °C/min ≥ 50 °C/min. Over the temperature range of 1400–1800 °C, with $P_S = 100$ MPa, $R_H = 50$ °C/min and $t_s < 20$ min, the grain grew uniformly, with distinct grain boundaries. The average size varied between 10 nm and 5 μm, yielding higher transmittance. Even under the aforesaid conditions except that under $t_s > 20$ min yielded slightly lesser transmittance due to the significant abnormal grain growth. Irrespective of the temperatures used for sintering > 1400 °C, when $t_s > 30$ min, the sintered samples cracks, as the average grain size increases over 20 mm. The aforesaid results clearly indicate that the optical transmittance of the ceramics does not completely rely on the grain size.

4. Conclusion

Transparent YLO ceramics with high density has been fabricated by SPS using the YLO powder synthesized by the co-precipitation method. The sintering parameters and their various effects on different factors of ceramics have been investigated. The complete densification was obtained at 1250 °C. Transparent YLO ceramics were obtained at $T_S = 1400$ °C ($t_s = 20$ min) and 1700 °C ($t_s = 5$ min) at 100 MPa, with $R_H = 50$ °C/min. A homogeneous microstructure was observed at 1400–1800 °C at $P_S = 100$ MPa with $t_s < 30$ min. The YLO ceramics fabricated at 1700 °C and 1400 °C had nearly 5–10% improvement in transmittance upon annealing at 1200 °C for 12 h. The discoloration disappears at annealing temperature of 1200 °C, compensating the oxygen vacancies, being the optimal temperature for post-annealing YLO ceramics. A high annealing temperature resulted in increase of pores and grain growth resulting in decrease in transmittance. We obtained nearly the similar transmittance as that was reported for HIP yielded YLO ceramics, with add on benefits like comparatively lesser temperature and short processing time. Further investigations on the grain boundaries and defects in the transparent ceramics of

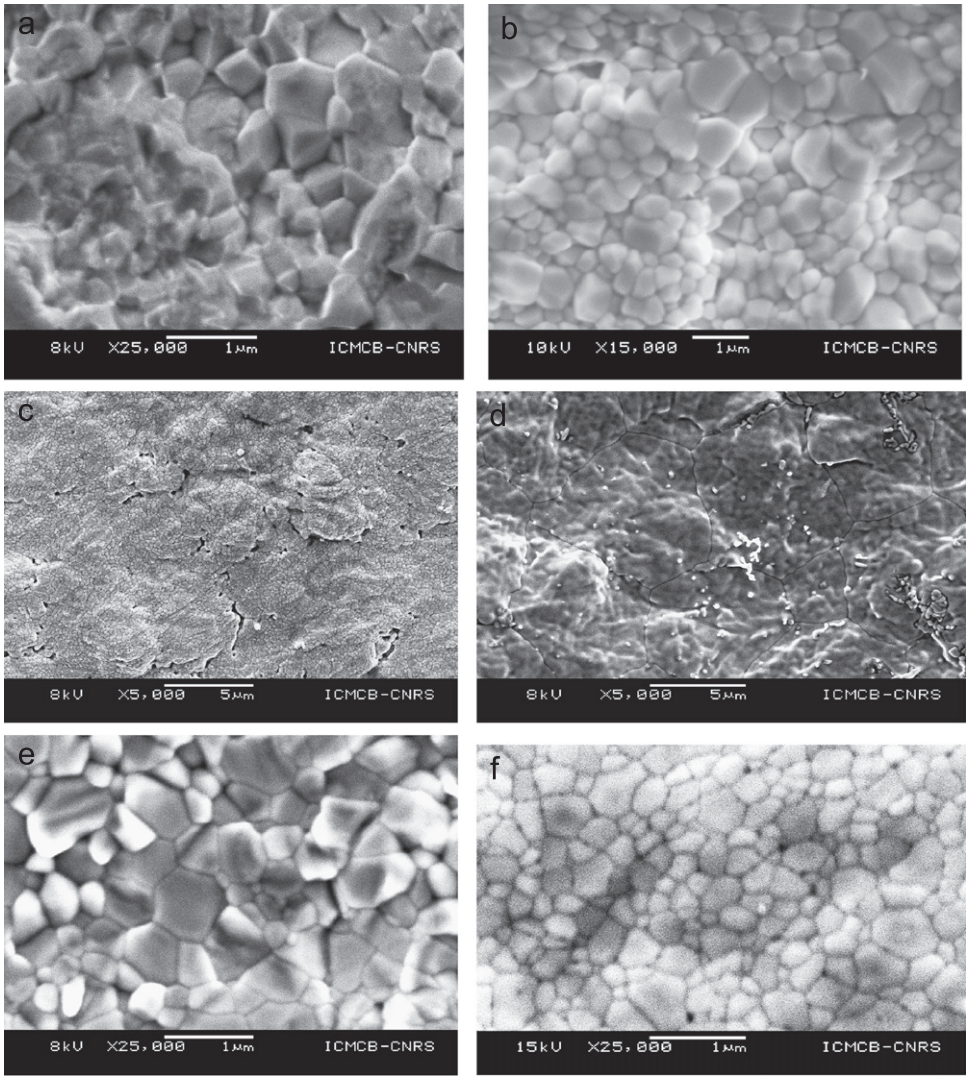

Fig. 5. SEM micrographs of ceramics: (a) 1500 °C, 100 MPa, t_s=5 min and R_H=50 °C/ min; (b) 1700 °C, 100 MPa, t_s= 5 min and R_H=50 °C/min; and (c) 1700 °C, 100 MPa, t_s= 5 min and R_H=50 °C/min, annealed at 1200 °C for 12 h.

YLO are in progress, which should enable us to increase the quality of the sintered ceramics by SPS for device applications.

Acknowledgment

The authors thank GIS-AMA (Advanced Materials in Aquitaine) for funding this project.

References

[1] C.R.E. Baer, C. Krankel, C.J. Saraceno, O.H. Heckl, M. Golling, R. Peters, K. Petermann, T. Sudmeyer, G. Huber, U. Keller, Femtosecond thin-disk laser with 141 W of average power, Optics Letters 35 (2010) 2302–2304.

[2] V. Peters, A. Bolz, K. Petermann, G. Huber, Growth of high-melting sesquioxides by the heat exchanger method, Journal of Crystal Growth 237 (2002) 879–883.

[3] K. Petermann, L. Fornasiero, E. Mix, V. Peters, High melting sesquioxides: crystal growth, spectroscopy, and laser experiments, Optical Materials 19 (2002) 67–74.

[4] R. Gaume, B. Viana, J. Derouet, D. Vivien, Spectroscopic properties of Yb-doped scandium based compounds Yb:$CaSc_2O_4$, Yb:$SrSc_2O_4$ and Yb:Sc_2SiO_5, Optical Materials 22 (2003) 107–115.

[5] R. Peters, C. Krankel, K. Petermann, G. Huber, Broadly tunable high-power Yb:Lu_2O_3 thin disk laser with 80% slope efficiency, Optics Express 15 (2007) 7075–7082.

[6] J.S. Sanghera, W. Kim, C. Baker, G. Villalobos, J. Frantz, B. Shaw, A. Lutz, B. Sadowski, R. Miklos, M. Hunt, F. Kung, I. Aggarwal, Laser oscillation in hot pressed 10%Yb^{3+}:Lu_2O_3 ceramic, Optical Materials 33 (2011) 670–674.

[7] K. Petermann, D. Fagundes-Peters, J. Johannsen, M. Mond, V. Peter, J.J. Romero, S. Kutovoi, J. Speiser, A. Giesen, Highly Yb-doped oxides for thin-disc lasers, Journal of Crystal Growth 275 (2005) 135–140.

[8] C.R. Bickmore, K.F. Waldner, D.R. Treadwell, R.M. Laine, Ultrafine spinel powders by flame spray pyrolysis of a magnesium aluminate double alkoxide, Journal of American Ceramic Society 79 (1996) 1419–1423.

[9] C. Hwang, T. Wu, J. Wan, Design and modify the combustion synthesis method to synthesize ceramic oxide powders, Journal of Materials Science 39 (2004) 4687–4691.

[10] L.A. Chick, L.R. Pederson, G.D. Maupin, J.L. Bates, L.E. Thomas, G.J. Exarhos, Glycine-nitrate combustion synthesis of oxide ceramic powders, Materials Letters 10 (1990) 6–12.

[11] Z.A. Munir, U. Anselmi-Tamburini, M. Ohyanagi, The effect of electric field and pressure on the synthesis and consolidation of materials: a review of the spark plasma sintering method, Journal of Materials Science 41 (2006) 763–777.
[12] C. Wang, Z. Zhao, Transparent $MgAl_2O_4$ ceramic produced by spark plasma sintering, Scripta Materialia 61 (2009) 193–196.
[13] B-N. Kim, K. Hiraga, K. Morita, H. Yoshida, Spark plasma sintering of transparent alumina, Scripta Materialia 57 (2007) 607–610.
[14] K. Morita, B-N. Kim, H. Yoshida, K. Hiraga, Spark-plasma-sintering condition optimization for producing transparent $MgAl_2O_4$ spinel polycrystals, Journal of American Ceramic Society 92 (2009) 1208–1216.
[15] Philippe Veber, Matias Velázquez, Véronique Jubera, Stanislav Péchev, Oudomsack Viraphong, Flux growth of Yb^{3+}-doped RE_2O_3 (RE=Y,Lu) single crystals at half their melting point temperature, Crystal Engineering Communications 13 (2011) 5220–5225.
[16] M. Galceran, M.C. Pujol, M. Aguilo, F. Diaz, Synthesis and characterization of nanocrystalline Yb:Lu_2O_3 by modified Pechini method, Materials Science Engineering B 146 (2008) 7–15.
[17] A. Ikesue, T. Kinoshita, K. Kamata, K. Yoshida, Fabrication and optical properties of high-performance polycrystalline Nd:YAG ceramics for solid-state laser, Journal of American Ceramic Society 78 (1995) 1033–1040.
[18] R. Chaim, M. Levin, A. Shlayer, C. Estournes, Sintering and densification of nanocrystalline ceramic oxide powders: a review, Advances in Applied Ceramics 107 (2008) 159–169.
[19] S. Hosokawa, H. Yagi, T. Yanagatani, Translucent Lutetium Oxide Sinter, and Method for Manufacturing Same, US Patent #7, 597 (2009) 866.
[20] I.W. Chen, X.H. Wang, Sintering dense nanocrystalline ceramics without final-stage grain growth, Nature 404 (2000) 168–171.
[21] X.H. Wang, P.L. Chen, I.W. Chen, Two-step sintering of ceramics with constant grain-size, I Y_2O_3, Journal of American Ceramics Society 89 (2006) 431–437.
[22] C-W. Li, S-C. Lui, J. Goldacker, Relation between strength, microstructure, and grain-bridging characteristics in *In Situ* reinforced silicon nitride, Journal of American Ceramics Society 78 (1995) 449–459.
[23] Z.J. Shen, M. Johnsson, Z. Zhao, M. Nygren, Spark plasma sintering of alumina, Journal of American Ceramics Society 85 (2002) 1921–1927.
[24] D.T. Jiang, D.M. Hulbert, U. Anselmi-Tamburini, T. Ng, D. Land, A.K. Mukherjee, Optically transparent polycrystalline Al_2O_3 produced by spark plasma sintering, Journal of American Ceramics Society 91 (2008) 151–154.
[25] E.A. Olevsky, S. Kandukuri, L. Froyen, Consolidation enhancement in spark-plasma sintering: impact of high heating rates, Journal of Applied Physics 102 (2007) 114913–114925.
[26] N. Murayama, W. Shin, Effect of rapid heating on densification and grain growth in hot pressed alumina, Journal of Ceramics Society Japan 108 (2000) 799–807.
[27] B-N. Kim, K. Hiraga, K. Morita, H. Yoshida, Effects of heating rate on microstructure and transparency of spark-plasma-sintered alumina, Journal of European Ceramics Society 29 (2009) 323–327.
[28] R. Chaim, A. Shlayer, C. Estournes, Densification of nanocrystalline Y_2O_3 ceramic powder by spark plasma sintering, Journal of European Ceramics Society 29 (2009) 91–98.
[29] Jianren Lu, T. Murai, K. Takaichi, T. Uematsu, K. Misawa, M. Prabhu, J. Xu, K. Ueda, H. Yagi, T. Yanagitani, A.A. Kaminskii, A. Kudryashov, 72 W Nd:$Y_3Al_5O_{12}$ ceramic laser, Applied Physics Letters 78 (2001) 3586–3588.